ISSN: 2994-7510

Review Article

Journal of Water Research

A Micro-Catchment Block-to-Inlet Framework for Diagnosing Nuisance Flood Failure Mechanisms under Dual Storm Typologies

Tefera Shibeshi[1*] and Temesgen Mekuriaw Manderso[2]

[1]*Department of Civil and Environmental Engineering ,Villanova university , PA, USA*

[2]*Department of Hydraulic and Water Resources Engineering, Debre Tabor University, Ethiopia.*

[*]Corresponding Author
Tefera Shibeshi, Department of Civil and Environmental Engineering ,Villanova university , PA, USA.

Submitted: 2026, Feb 02; **Accepted:** 2026, Mar 03; **Published:** 2026, Mar 12

Citation: Tefera. S., Temesgen. M. M. (2026). A Micro-Catchment Block-to-Inlet Framework for Diagnosing Nuisance Flood Failure Mechanisms under Dual Storm Typologies. *J Water Res, 4*(1), 01-13.

Abstract

Urban neighborhoods, such as Kensington in Philadelphia, frequently encounter nuisance flooding, which is characterized by shallow surface ponding around street inlets during moderate rainfall events. These recurrent low-depth floods disrupt mobility, damage infrastructure, and disproportionately impact vulnerable communities, often occurring below conventional stormwater design thresholds. This study introduces an uncalibrated, diagnostic micro-catchment block-to-inlet modeling framework aimed at identifying localized hydraulic failure mechanisms, rather than replicating observed flood depths. High-resolution elevation data and parcel-scale impervious surface mapping were employed to delineate inlet-based micro-catchments, each approximately 5 ha in size. These micro-catchments were integrated into a comprehensive EPA SWMM (v5.2) hydraulic-hydrologic model of a 3.5 km² urban drainage network located in Kensington, Philadelphia, USA. Two synthetic storm typologies were utilized to isolate contrasting failure modes: (i) a short-duration, high-intensity convective storm representing peak-limited conditions and (ii) a long-duration, high-volume frontal storm representing volume-driven surcharge. The findings suggest that short-duration intense storms lead to rapid inlet exceedance and transient hydraulic instability, whereas long-duration storms result in sustained system pressurization and prolonged surface flooding. In both storm scenarios, a consistent set of junctions and downstream corridors emerged as significant structural bottlenecks, with limited external discharge capacities constraining system performance. Although the framework is not calibrated to observed events, it offers actionable diagnostic insights into inlet-scale vulnerabilities and supports targeted infrastructure upgrades and real-time flood management strategies in densely populated urban neighborhoods.

Keywords: Nuisance Flooding, Micro-Catchment Hydrology, SWMM Diagnostics, Inlet-Scale Failure, Urban Drainage Systems, Storm Typology

1. Introduction

Nuisance flooding, characterized by the shallow accumulation of stormwater at street inlets and in urban depressions during moderate rainfall events, presents an increasingly significant challenge in densely populated urban neighborhoods, such as Kensington in Philadelphia. These low-depth, high-frequency events, distinct from riverine or coastal flooding, disrupt mobility, damage parked vehicles and building foundations, exacerbate basement seepage, and disproportionately affect economically vulnerable communities with limited adaptive capacity [1]. Notably, nuisance flooding often occurs when rainfall intensities remain below conventional design thresholds (e.g., 10-year storms), highlighting the limitations of traditional stormwater design and evaluation approaches [2].

Recent advancements in urban hydrology indicate that nuisance flooding is predominantly influenced by micro-scale hydrologic and hydraulic processes at the parcel- and block-level scales rather than by larger catchments encompassing tens of hectares. LiDAR-based micro-topographic analyses have revealed that

subtle elevation gradients, curb alignments, and roof drainage pathways significantly affect localized runoff routing, thereby elucidating the recurrent flooding observed at specific intersections despite spatially uniform rainfall [3]. Furthermore, the hydraulic performance at the inlet scale is crucial for determining whether street runoff is captured or bypassed, with the inlet efficiency being highly sensitive to flow depth, debris accumulation, and inlet geometry [4,5].

The structure of storms significantly influences the mechanisms of nuisance flooding. Short-duration convective storms produce rapid peak discharges that can exceed inlet capacity, whereas long-duration frontal systems exert sustained hydraulic stress, resulting in prolonged surcharges and surface ponding, even at moderate intensities. Differentiating between peak-limited and volume-driven failure modes is crucial for identifying system vulnerabilities and developing effective mitigation strategies.

This study addressed the limitations inherent in coarse-scale urban drainage modeling by introducing a micro-catchment block-to-inlet diagnostic framework. This framework explicitly delineates the runoff contributions of individual parcels and blocks to specific inlet structures. By integrating fine-scale topography with dynamic hydraulic routing within the SWMM, the framework facilitates the systematic identification of failure mechanisms at both the inlet and network scales under varying storm structures. The primary objective was not to predict flooding events but to diagnose structural vulnerabilities within the system under controlled storm typologies. This approach supports targeted infrastructure planning and real-time flood management in densely populated urban areas.

2. Materials and Methods

This study utilizes an uncalibrated yet structurally consistent hydraulic–hydrologic modeling framework to assess system vulnerabilities under varying storm structures. Model parameters were chosen to reflect typical urban drainage conditions based on existing literature and design standards, rather than to replicate a specific observed flood event. The focus is on relative system response, spatial failure patterns, and predominant hydraulic mechanisms, rather than on absolute flood depths or the precision of discharge predictions.

2.1. Study Area Characterization

The study area encompasses approximately 3.5 km² of the Kensington neighborhood in Philadelphia, Pennsylvania, which has been delineated into inlet-based micro-catchments using high-resolution elevation data and street geometry. This area is characterized by dense residential development, mixed land use, and an average impervious surface fraction of approximately 55%, with drainage connectivity directed toward clustered street outlets. The frequent occurrence of nuisance flooding during moderate rainfall events renders Kensington an appropriate case study for examining the inlet-scale hydrologic responses and micro-catchment dynamics. Furthermore, the neighborhood exemplifies legacy combined-sewer districts common in older U.S. cities, thereby enhancing the applicability of the findings.

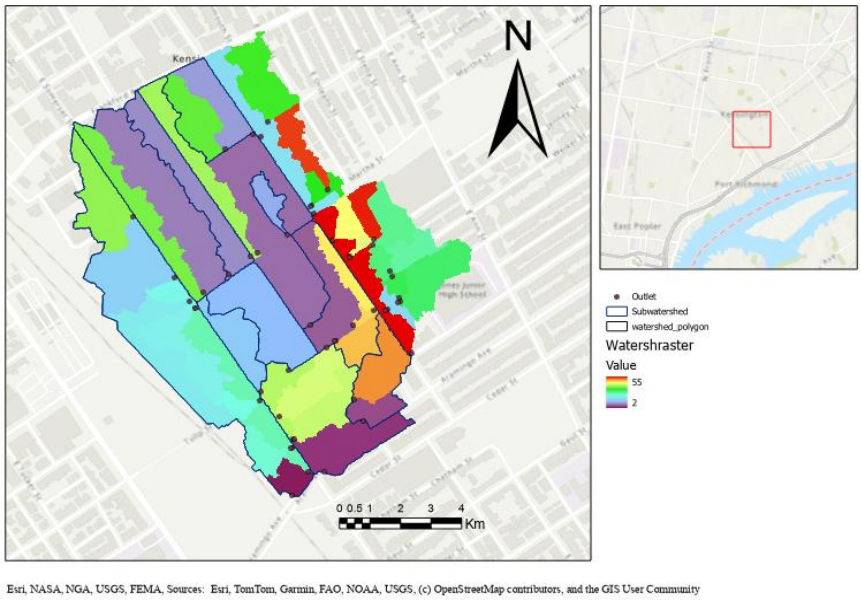

Figure 1: Micro-Catchment Delineation for the Kensington Study Area in Philadelphia

2.2. Data Sources and Preprocessing

A comprehensive compilation of hydrometeorological, geospatial, and infrastructure datasets was assembled (Table 1). These datasets were integrated within ArcGIS Pro 3.0 using standard geoprocessing workflows: (1) DEM-based flow accumulation and flow direction analyses using the D8 algorithm to delineate micro-catchment boundaries; (2) overlay of inlet point features to assign outlet nodes; (3) calculation of catchment areas, slopes, and percent imperviousness from building footprint vectors.

Data Type	Description	Source	Resolution/Format	Application
Rainfall events	Event-based precipitation time series (Storm A: 62.48 in.; Storm B: 115.82 in.)	Burn et al. (2025)	1-minute intervals	SWMM rainfall input
Digital Elevation Model	High resolution DEM	USGS 3DEP	1 m raster	Micro-catchment delineation
Building footprints	Vector polygon outlines of structures	OpenDataPhilly	Vector (polygon)	Imperviousness calculation
Land use / cover	Classification raster (residential, commercial, impervious, pervious)	OpenDataPhilly / NLCD	Vector and raster	Catchment characterization
Street network	Street centerlines and road geometry	OpenDataPhilly	Vector (polyline)	Network topology
Stormwater inlets	Point locations of curb, grate, and combination inlets	OpenDataPhilly	Vector (point)	Outlet node assignment

Table 1: Data Sources and Specifications

2.3. SWMM Model Setup and Configuration

2.3.1. Hydrologic and Hydraulic Framework

The EPA Storm Water Management Model (SWMM v5.2) was configured to simulate runoff generation and hydraulic routing from 29 inlet-based micro-catchments under controlled-storm inputs. All hydrologic and hydraulic parameters, including sub-catchment areas, slopes, Manning's roughness coefficients, infiltration parameters, and conduit geometry, were held constant across simulations to isolate the influence of storm temporal structure on system response. This controlled configuration enables a direct comparison of peak-limited and volume-driven failure mechanisms, independent of parameter tuning or calibration effects.

2.3.2. Sub catchment Definition and Infiltration Modeling

Each sub-catchment was allocated a uniform total imperviousness of 55%, in accordance with the parcel-scale land-cover analysis. Of this imperviousness, approximately 25% was designated as a directly connected impervious area, contributing to immediate runoff, while the remaining impervious and pervious portions were subject to infiltration losses.

The Horton method was employed to represent infiltration, utilizing an *initial infiltration rate of 6.0 in·hr⁻¹, a final infiltration rate of 0.5 in·hr⁻¹*, and *a decay coefficient of 4.0 day⁻¹*. These values are consistent with those reported for moderately compacted urban soils in residential settings. The parameters were selected from established ranges in the literature and were not calibrated to site-specific field measurements in accordance with the diagnostic objectives of the study. Infiltration was applied exclusively to pervious surfaces, whereas directly connected impervious areas contributed all incident rainfall to runoff.

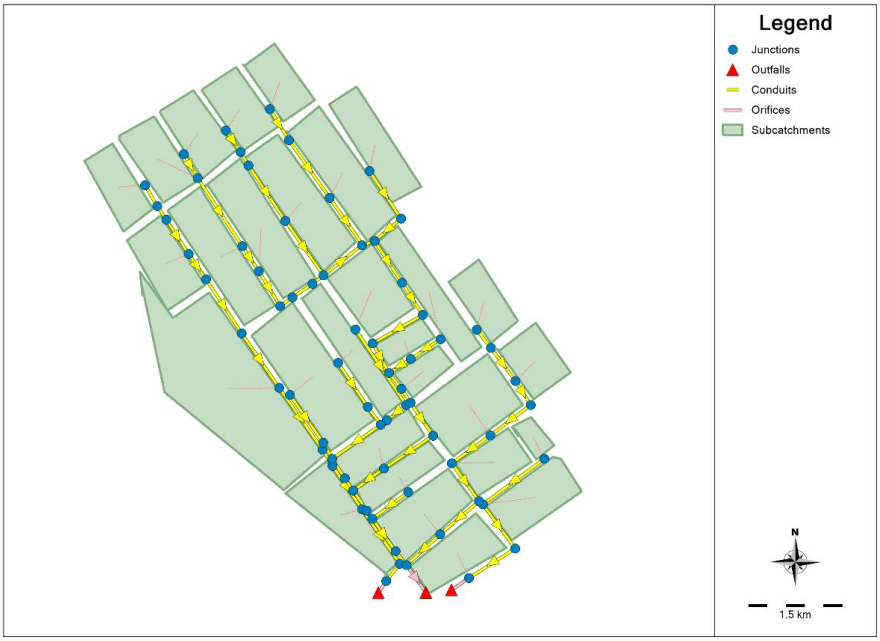

Figure 2: SWMM Model Configuration

2.3.3. Network Topology: Nodes and Links

The drainage network included 72 junction nodes (3 outfalls) and 69 circular conduits forming the local combined sewer system. Most conduits are 18 in. diameter, with lengths and slopes from GIS and design records. Some downstream links had low or adverse slopes, causing backwater effects and surcharges during storms. The system's only external discharge points are three orifice-controlled outfalls, which act as primary bottlenecks. Each sub catchment outlet connected to a junction node representing a street inlet, linking surface runoff to subsurface flow.

2.3.4. Numerical Solution and Routing Method

Dynamic wave routing was employed to solve the full Saint-Venant equations, facilitating the representation of backwater effects, pressurized flow, and rapid hydraulic transitions characteristic of urban-drainage networks under surcharge conditions. A base computational time step of one minute was used, with adaptive reduction during high-gradient conditions to ensure numerical stability. This methodology prioritizes the accurate depiction of hydraulic regime transitions over computational efficiency.

2.4. Storm Typology Scenarios

Two synthetic storm typologies were employed to identify the primary mechanisms of nuisance flooding failure, in accordance with the storm structure classification framework established by Burns et al [6]. Instead of replicating specific historical events, storm depths and intensities were deliberately adjusted to test system capacity and uncover structural vulnerabilities under varying temporal rainfall patterns.

Storm A exemplified a short-duration, high-intensity convective event characteristic of summer thunderstorms in the Mid-Atlantic region, resulting in rapid peak inflows within a timeframe of less than three hours. In contrast, Storm B represented a long-duration frontal or tropical-remnant system, marked by sustained moderate rainfall over approximately 12–14 h, thereby generating substantial cumulative runoff volumes. Both meteorological events were analyzed under saturated antecedent conditions to emphasize the response of the drainage system rather than variations in soil moisture.

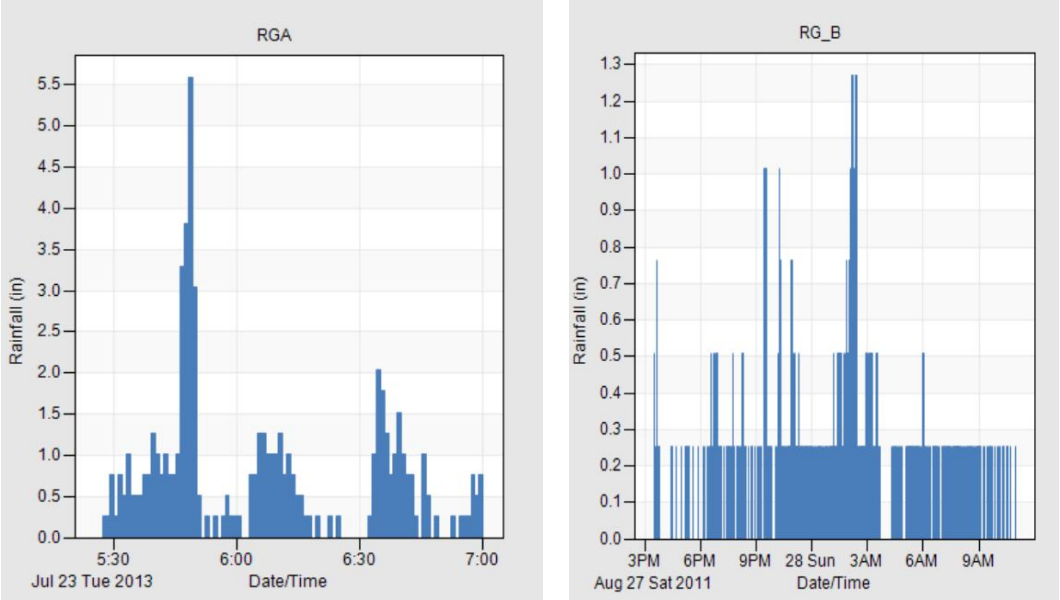

Figure 3: Hyetograph for Storm A and Storm B

3. Results

3.1. Storm A: Short-Intense Simulation Results

3.1.1. Runoff Generation and Continuity

Storm A elicited a swift hydrologic response across the 145-hectare study area, which is characteristic of a short-duration, high-intensity convective rainfall event. Most of the precipitation was converted to surface runoff, with only a minor portion lost to infiltration due to saturated antecedent conditions and the limited duration of the storm. This behavior exemplifies a peak-dominated runoff regime, in which the rainfall intensity surpasses the infiltration capacity early in the event. Overall hydrologic continuity was preserved, with mass balance errors remaining below 1%, indicating internally consistent model accounting. Given the diagnostic purpose of the simulations, continuity metrics were interpreted as indicators of numerical stability rather than as validation against observed flows.

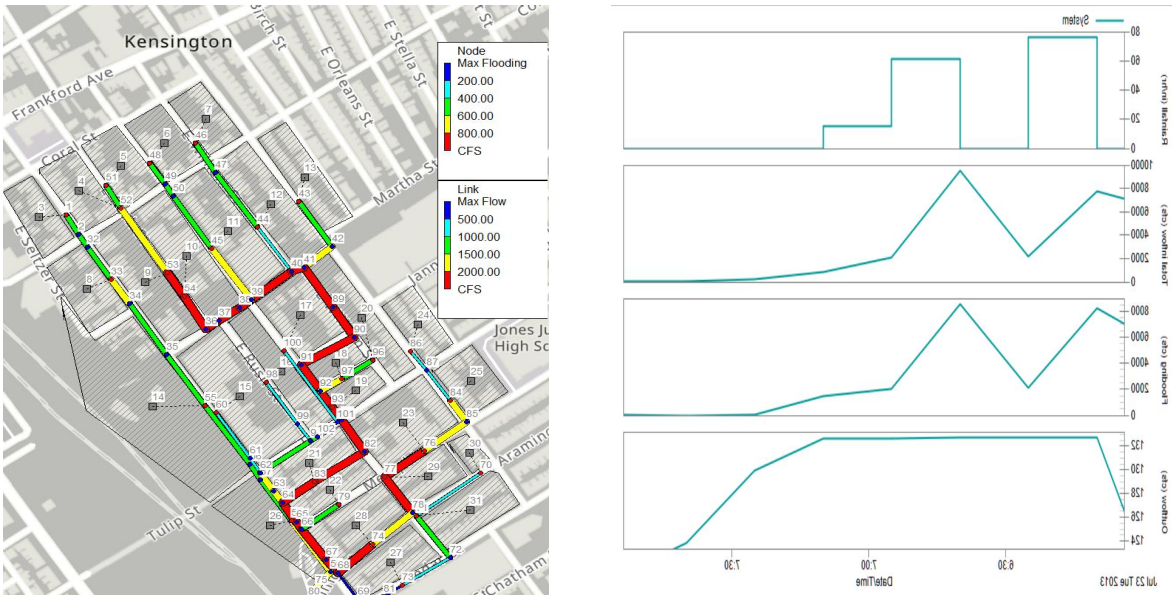

Figure 4: Catchment Rainfall Runoff Response

3.1.2. Flow Routing and System Hydraulics

Analysis of routing results reveals that the drainage network was subjected to significant hydraulic stress under the conditions of ***Storm A.*** A substantial portion of the generated runoff cannot be accommodated by the sewer system, resulting in surface flooding. This outcome reflects the rapid exceedance of the inlet capacity and limitations in downstream conveyance. Minimal external discharge through the three outfall structures suggests that the system performance was primarily governed by downstream controls rather than the supply of upstream runoff. The hydraulic response was marked by swift transitions between the *free surface* and *pressurized flows*, particularly within the interior grid nodes and downstream corridors. These transient conditions are indicative of peak-limited failure, wherein short-duration inflow surges exceed the capacity of the inlets and conduits before the downstream storage or discharge mechanisms can effectively respond.

Dynamic Wave routing required highly refined time-stepping under transient surcharging conditions and its performance shown below:

Metric	**Value**
Average routing time step	15.91 seconds
Minimum routing time step	0.84 seconds
Percent of non-converging steps	71.9%
Non-convergence interpretation	Rapid HGL fluctuations, multiple surcharged nodes

The high rate of non-converging time steps (71.9%) indicates that the hydraulic system experienced severe transient behavior rapid transitions between free-surface and pressurized flow, HGL oscillations, and momentum exchange typical of peak-limited surcharge under extreme rainfall.

3.1.3. Node-Scale Flooding and Continuity

During Storm A, flooding was predominantly concentrated within the interior grid nodes and the southern outflow corridor, which corresponded to regions characterized by limited slope and converging upstream inflows. Nodes displaying elevated continuity deviations were consistently aligned with known hydraulic bottlenecks, where rapid inflow convergence surpassed the downstream conveyance capacity as shown in Fig.5. The elevated continuity errors observed at these nodes were interpreted as indicators of localized hydraulic imbalance under extreme transient loading rather than numerical failure. These locations represent points where rapid changes in the hydraulic grade line and momentum exchange result in short-lived storage discrepancies under peak inflow conditions.

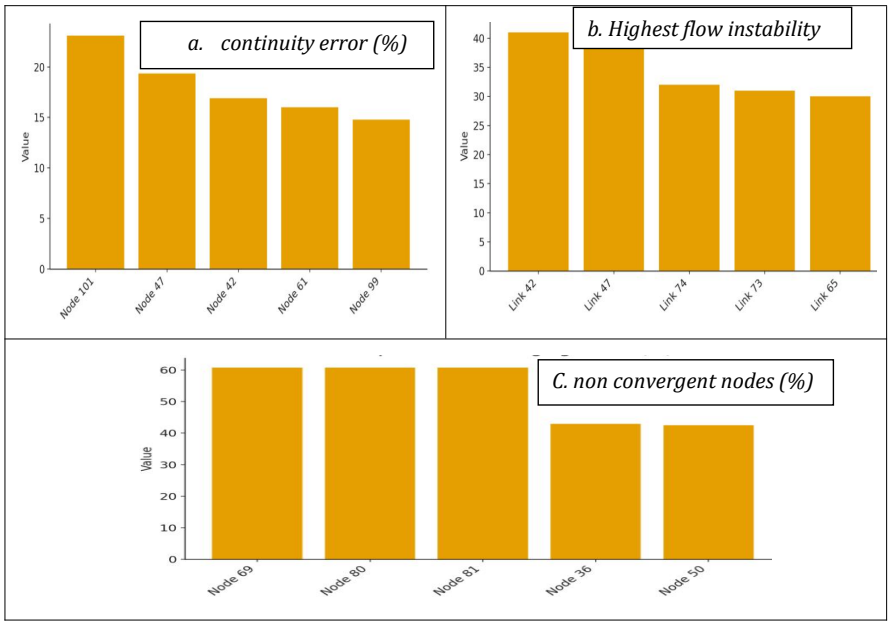

Figure 5: Storm A Node Scale Flooding and Continuity

Flooding extent and severity exhibited clear spatial patterns aligned with topography and pipe capacity as presented below:

3.1.4. Temporal Dynamics and Peak Flooding

Peak flooding was observed within the initial 30 min of Storm A, which aligned with the period of maximum rainfall intensity and rapid inflow concentration. Flood volumes increased sharply and then receded gradually after the cessation of rainfall, resulting in an asymmetric flood response typical of peak-limited systems. This temporal pattern indicates the inability of downstream controls to swiftly evacuate inflows during short-duration convective storms, even when the total rainfall volume is relatively modest.

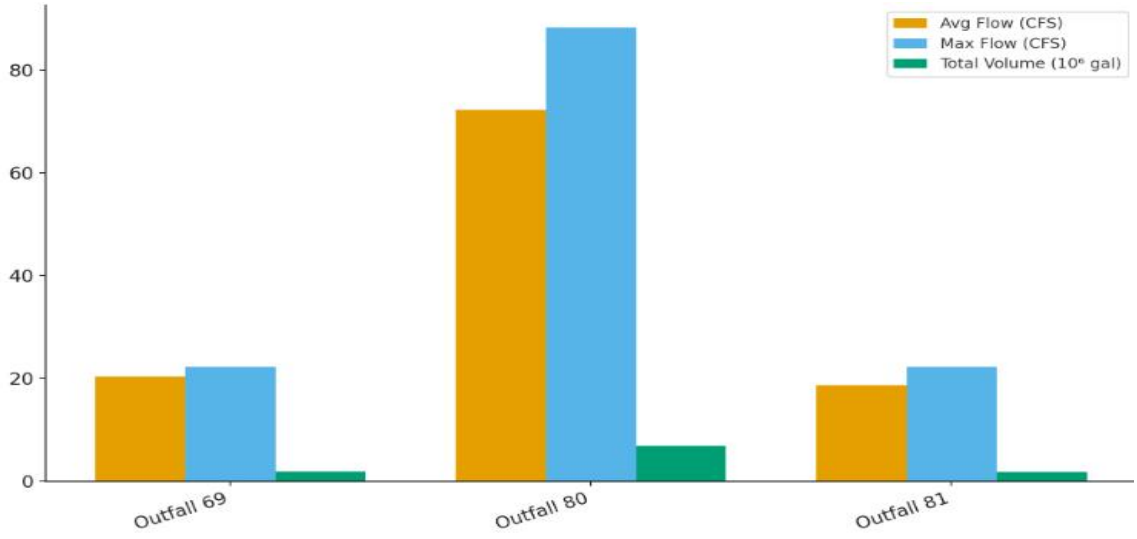

Figure 6: Storm A outfall Loading Summary

3.2. Storm B: Long-Duration, High-Volume Simulation Results

3.2.1. Runoff Generation and Hydrologic Response

Storm B illustrated (Fig.7) a sustained hydrologic response, primarily influenced by the duration of rainfall rather than its peak intensity. Despite an increase in infiltration losses compared to Storm A, the extended duration of rainfall resulted in significantly higher cumulative runoff volume. This response exemplifies a volume-driven regime, wherein the system performance is dictated by the exhaustion of storage capacity and prolonged surcharge, as opposed to short-term inflow exceedance. Throughout the simulation, hydrologic continuity remained robust, indicating a stable mass balance under quasi-steady, pressurized conditions.

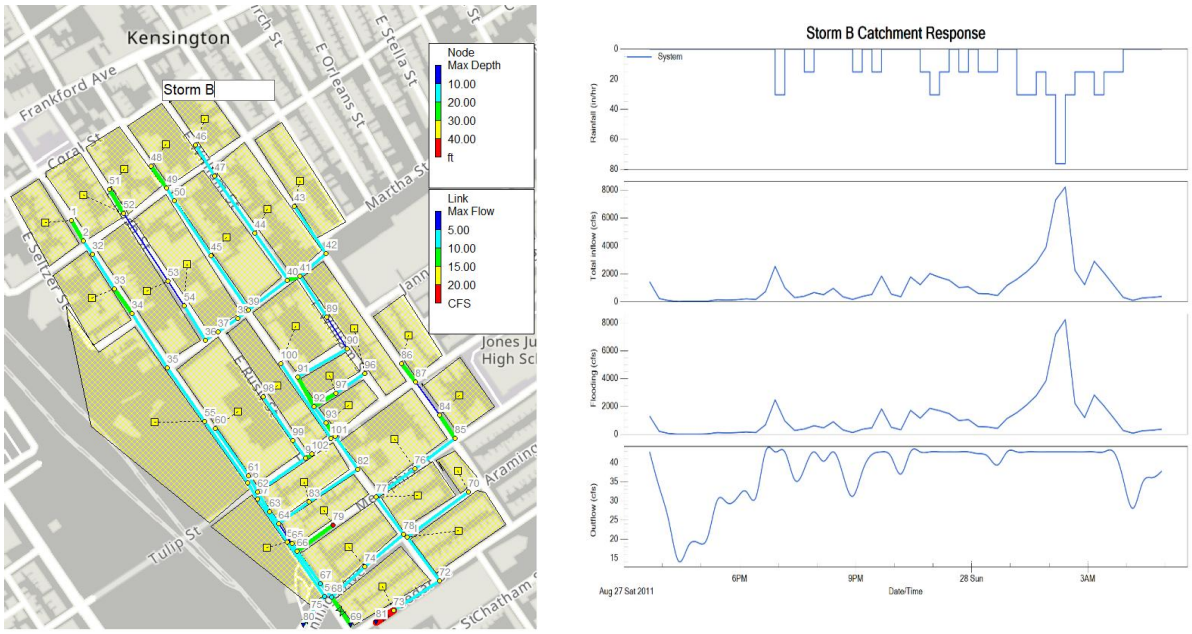

Figure 7: Storm B Response and Hydrologic Response of System

3.2.2. Flow Routing Performance and System Saturation

Routing analyses reveal that the drainage system swiftly transitioned into a state of sustained surcharge during Storm B. Once pressurized, the network remained hydraulically saturated for the majority of the storm duration, exhibiting limited capacity to store or discharge incoming flows. Consequently, surface flooding persisted throughout the event and gradually receded after the cessation of rainfall. In contrast to Storm A, the hydraulic gradients evolved gradually, resulting in smoother transitions and enhanced numerical stability. This behavior underscores the fundamentally different failure mechanism associated with long-duration rainfall, wherein the cumulative volume, rather than the peak inflow, dictates the system's response.

Under long-duration sustained surcharge, the Dynamic Wave solver exhibited improved stability as presented below.

Metric	Value
Average routing time step	19.87 seconds
Percent of time steps at maximum allowable step (20 sec)	99.35%
Non-converging steps	<1%
Interpretation	Smooth, quasi-steady hydraulic regime despite large surcharge volumes

The contrast with Storm A is instructive: whereas brief intense rainfall creates transient shock fronts and rapid regime transitions (causing solver non-convergence), sustained rainfall at moderate intensity produces a smoother, more gradually evolving pressure field that the Dynamic Wave solver can track accurately with relatively large time steps.

3.2.3. Node-Scale Stability and Continuity Errors

Node-level diagnostics indicated that although Storm B resulted in larger cumulative flooding volumes, it produced smaller continuity deviations at critical nodes than Storm A. This suggests a hydraulically stable, capacity-constrained system functioning under sustained pressurization. The recurrence of the same critical nodes across both storm types highlights the structural nature of network vulnerabilities, irrespective of the temporal structure of the storm.

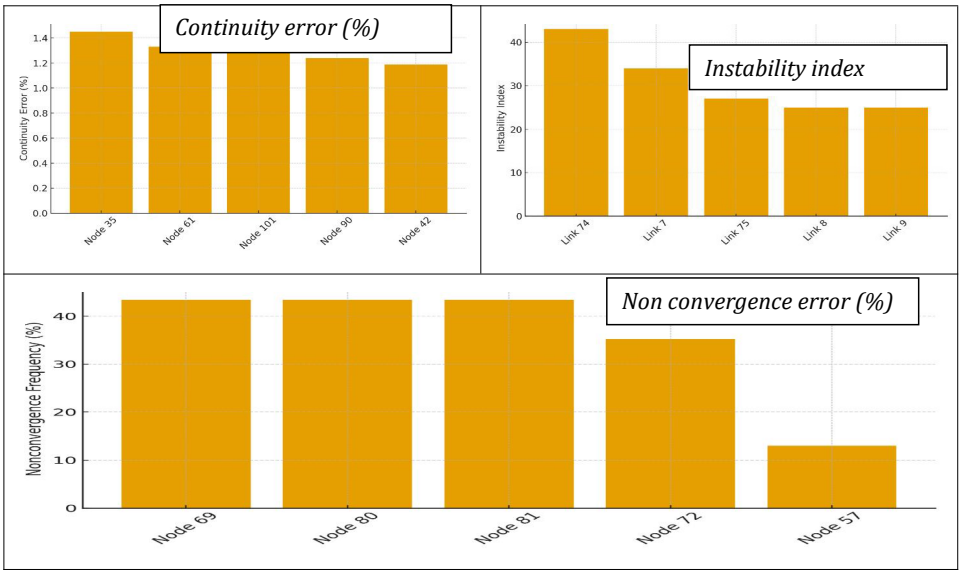

Figure 8: Node Scalability and Continuity Error

3.2.4 Peak Flooding Timing and Hydrograph Characteristics

During Storm B, peak flooding was observed early in the simulation; however, it persisted throughout the entire rainfall duration, resulting in an extended flooding plateau rather than a distinct peak. This sustained inundation indicates a volume-driven failure mode, in which surcharged pipes impede effective drainage even after the intensity of the rainfall diminishes.

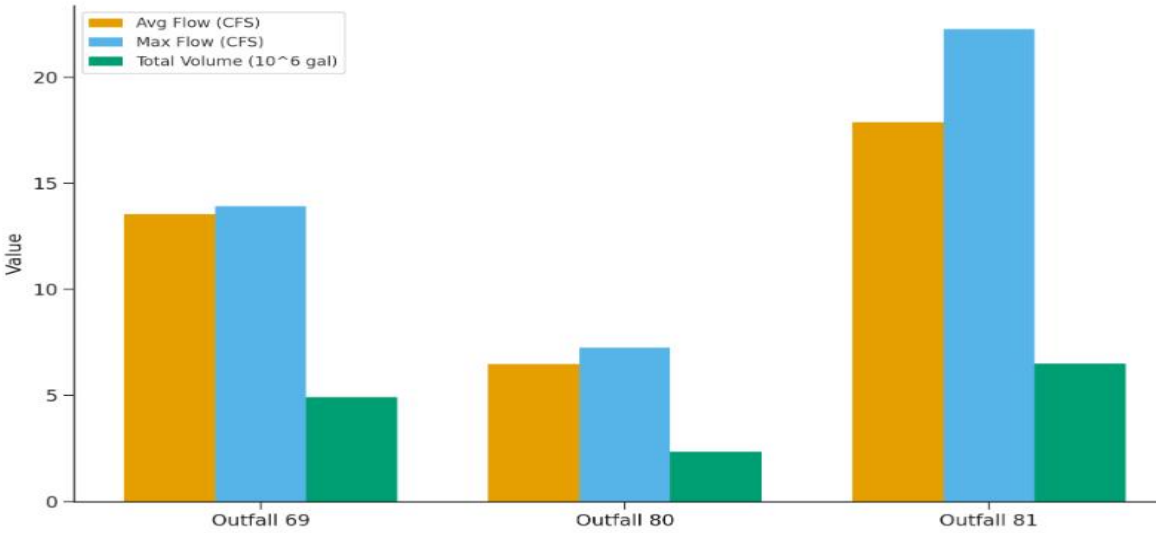

Figure 9: Storm B Outfall Loading Summary

4. Discussion

4.1. Comparative Analysis: Storm A vs. Storm B

The divergent responses observed under Storms A and B elucidate two fundamentally distinct nuisance flooding failure mechanisms within the Kensington drainage network. Short-duration convective storms (Storm A) induced peak-limited failure, characterized by rapid inflow surges that surpassed the inlet and conduit capacity before the downstream discharge could be adjusted. These conditions resulted in abrupt hydraulic transitions, transient pressurization, and flooding concentrated within the first hour of rainfall. Conversely, long-duration frontal storms (Storm B) caused volume-driven failure, wherein sustained inflow progressively saturated the drainage system, leading to prolonged surcharges and extended surface flooding. Although the hydraulic conditions under Storm B were numerically more stable, the system's inability to evacuate cumulative runoff volumes resulted in substantially longer inundation periods. Both storm types consistently identified the same critical nodes and corridors

as dominant constraints, indicating that nuisance flooding in Kensington is primarily governed by structural network limitations rather than storm-specific variability. This finding suggests that targeted infrastructure interventions can mitigate multiple storm failure modes.

4.2. System-Level Constraints and Hydraulic Vulnerabilities

4.2.1. Downstream Discharge Capacity

Both storm simulations demonstrated a significantly restricted external discharge capacity, with only a minimal proportion of the system inflow being discharged through the three outfall structures. This suggests that downstream controls serve as primary bottlenecks, thereby constraining the overall system throughput, irrespective of upstream runoff generation mechanisms. In optimally functioning urban drainage systems, a considerable portion of inflow is typically directed through primary outlets during storm events, with temporary storage to accommodate the remainder. The persistently low discharge observed in this study implies that the outfall orifices are either undersized relative to the system inflows or are affected by downstream backwater effects. Consequently, enhancing downstream discharge capacity has emerged as a strategic intervention with the potential to mitigate nuisance flooding in both peak-limited and volume-driven storm scenarios.

4.2.2. Pipe Slope and Conduit Design Constraints

Numerous conduits within the network exhibit minimal gradients or adverse hydraulic profiles, rendering these segments susceptible to backwater effects, sediment accumulation, and prolonged surcharges during wet weather conditions. Pipes with low gradients are particularly prone to oscillatory pressurization and momentum reversal once the downstream capacity is exceeded, thereby exacerbating upstream flooding even under moderate inflows. These observations align with the challenges frequently encountered in aging combined sewer systems, where outdated design standards and long-term sedimentation diminish effective conveyance capacity. Remedial measures, such as profile re-grading, selective pipe replacement, or the incorporation of inline storage, could significantly enhance hydraulic stability in these critical segments.

4.2.3. Inlet Density and Surface Runoff Pathways

The micro-catchment framework underscores the significance of inlet density in regulating surface runoff concentrations at the block scale. Under peak intensity conditions, individual micro-catchments produce substantial short-term inflows that may surpass the inlet capture capacity, thereby contributing to localized ponding. Enhancing the inlet density can mitigate peak loading at individual inlets and improve the spatial distribution of inflows. However, the findings also indicate that improvements at the inlet level alone are inadequate when downstream conveyance remains limited. Without corresponding enhancements in trunk capacity or outlet discharge, additional inlets may only expedite surcharge propagation within the network. Therefore, effective mitigation necessitates a coordinated approach that considers inlet spacing, pipe capacity, and downstream controls.

4.3. Implications for Real-Time Flood Monitoring and Prediction

The diagnostic framework developed in this study has significant implications for real-time flood monitoring and operational decision-making. By identifying specific blocks and nodes that consistently experience surcharges under various storm typologies, municipal agencies can prioritize pre-storm interventions such as inlet clearing, debris removal, and temporary protective measures. Moreover, the strategic deployment of water-level sensors at critical nodes would facilitate the real-time integration of hydraulic conditions into a digital representation of SWMM, thereby enhancing situational awareness during storm events. Although not designed as a predictive forecasting tool in its current form, the framework establishes a foundation for adaptive operational strategies that mitigate the impacts of nuisance flooding through informed and timely interventions.

5. Conclusion

This study illustrates the effectiveness of a micro-catchment block-to-inlet diagnostic modeling framework in identifying the failure mechanisms associated with nuisance flooding in densely populated urban drainage systems. By explicitly connecting parcel-scale runoff generation to inlet-level hydraulic responses, the framework uncovers system vulnerabilities that remain undetected in traditional coarse catchment models. A comparative analysis of the two contrasting storm typologies revealed distinct yet complementary failure modes. Short-duration, high-intensity storms result in peak-limited inlet failures, characterized by rapid surcharges and localized flooding, whereas long-duration storms lead to volume-driven system saturation, causing prolonged surface inundation. Despite these differences, both storm types consistently identified the same downstream corridors and junctions as primary structural constraints, emphasizing the importance of network configuration over storm-specific variability. The findings indicate that severely restricted downstream discharge capacity constitutes the most critical system-level bottleneck, limiting performance under both peak- and volume-driven conditions. Micro-catchment delineation further highlights the impact of localized topography, inlet spacing, and low-slope conduits on the patterns of nuisance flooding. Although the model was not calibrated to observed flood events, this study offers actionable diagnostic insights that can guide targeted infrastructure upgrades, sensor placement, and operational preparedness strategies. The proposed framework is applicable to other densely populated urban neighborhoods and provides a scalable approach for more resilient, data-informed stormwater management.

Limitations

This study has several limitations that must be considered when interpreting the results. First, elevation data, pipe inverts, and inlet locations were sourced from available GIS datasets, which may not accurately represent current field conditions, such as undocumented infrastructure modifications, sediment accumulation, or partial inlet blockages. Second, infiltration was modeled using the Horton method with uniform parameters selected from published urban soil ranges. The model did not explicitly account for the spatial

variability of soil texture, groundwater conditions, and seasonal moisture dynamics. Third, the study assumed an ideal inlet capture efficiency, with all runoff reaching an inlet entering the subsurface system. In practice, the inlet efficiency is influenced by factors such as depth, debris accumulation, and inlet geometry, which can lead to bypass flows that are not represented in this model. Fourth, conduit roughness values were held constant across the network, despite known variability due to pipe material, age, biofilm development, and sediment deposition. Increased roughness in low-slope conduits further reduces the conveyance capacity. Fifth, downstream boundary conditions were simplified using fixed outfall orifice representations, whereas real-world performance is affected by the receiving water stage, tidal effects, and backwater from larger systems. Finally, the SWMM was not calibrated against the observed flow or flood depth data. Consequently, the findings should be interpreted as relative diagnostics of system behavior and failure mechanisms rather than absolute predictions of flood magnitude or extent [7].

References

1. Jiang, Y., Liu, Y., & Liang, S. (2020). Vulnerability assessment of urban flood disaster in coastal megacities: A case study of Shanghai. *Journal of Cleaner Production, 267,* 122–143, (2026).
2. Ozdemir, H., Erpul, G., & Ocakoglu, F. (2022). Nuisance flooding and urban resilience in low-lying coastal neighborhoods. *Environmental Science & Technology, 56*(12), 8541–8559, (2026).
3. Wang, M., Mao, Z., & Jia, H. (2021). The role of micro-topography in urban flood risk assessment: A LiDAR-based analysis. *Water Resources Management, 35*, 2691–2705,(2026).
4. Russo, B., Casas, M. R., & Mozzo, A. (2021). Hydraulic performance of urban drainage inlets: Full-scale laboratory experiments and field validation. *Water Resources Management, 35*, 1345–1365, (2026).
5. Okeya, O. N., Afolayan, O., & Dutta, S. (2022). Experimental evaluation of inlet capture efficiency under clogging conditions. *Journal of Environmental Engineering, 148*(5), 04022014, (2026).
6. Burns, M. J., & Good, K. D. (2025). Objective Air Mass Partitioning of Historical Rainfall for Informing Hydrologic Analysis and Design. *Journal of Hydrologic Engineering, 30*(6), 05025015.
7. U.S. Environmental Protection Agency. (2017). *Storm Water Management Model (SWMM) Reference Manual, Version* 5.1. EPA Office of Research and Development, Cincinnati, OH.

Appendix

Storm A

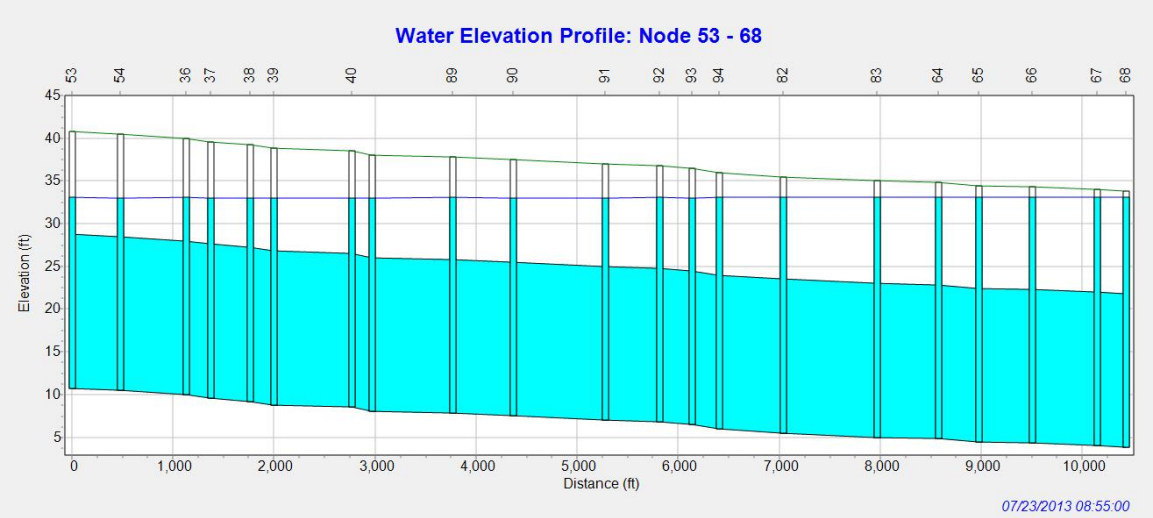

Figure 1A: Sample Profile of the Storm Type A

Rank	Node ID	Continuity Error (%)	Max Inflow (CFS)	Invert Elev. (m)	Interpretation
1	101	23.29	1,499.32	6.20	Extreme surcharge; flow convergence bottleneck from multiple upstream links
2	47	19.16	1,279.86	9.20	High interior-block accumulation; limited downstream capacity
3	42	17.24	2,138.44	8.40	Severe overflow; bottleneck between multiple sub-grid flows
4	61	15.73	898.76	5.20	Downstream surcharge propagation; minor continuity deviation
5	99	14.70	1,530.81	6.00	Persistent overflow during peak rainfall; eastern block accumulation

Table 3.1: Nodes with Highest Continuity Errors (Storm A)

Rank	Link ID	From Node	To Node	Instability Index	Length (m)	Slope (%)	Max Flow (CFS)	Interpretation
1	73	101	102	50	395	0.1215	1,166	Severe HGL oscillations; incoming flow reversal due to backwater
2	42	59	75	47	343	0.2915	1,531	Steep conduit with upstream surcharge; transient momentum effects
3	2	2	32	46	250	0.2400	1,048	High slope but limited upstream capacity; rapid filling-emptying cycles
4	18	49	50	46	242.7	0.1648	1,197	Steep, short conduit; backwater from downstream constraints
5	47	79	66	45	701	0.0285	1,177	Gentle slope; insufficient capacity for concentrated peak flow

Table 3.2: Conducts with Highest Hydraulic Instability (Storm A)

Node ID	Non-Converging Time Steps (%)	Type	Max Depth (m)	Invert Elev. (m)	Implication
80	71.89	OUTFALL	0.00	1.20	Severe surcharge in upstream path; extreme transient behavior
69	71.89	OUTFALL	0.00	2.50	High-flow convergence zone; rapid upstream-downstream decoupling
81	71.89	OUTFALL	0.00	2.60	Junction of multiple high-inflow conduits; local resonance effects
86	43.65	JUNCTION	30.00	6.50	Moderate instability; downstream backwater propagation
87	43.28	JUNCTION	30.00	6.00	Moderate instability; pressure fluctuations from orifice outlet constraints

Table 3.3: Nodes with Highest Non-Convergence Frequency (Storm A)

Storm B:

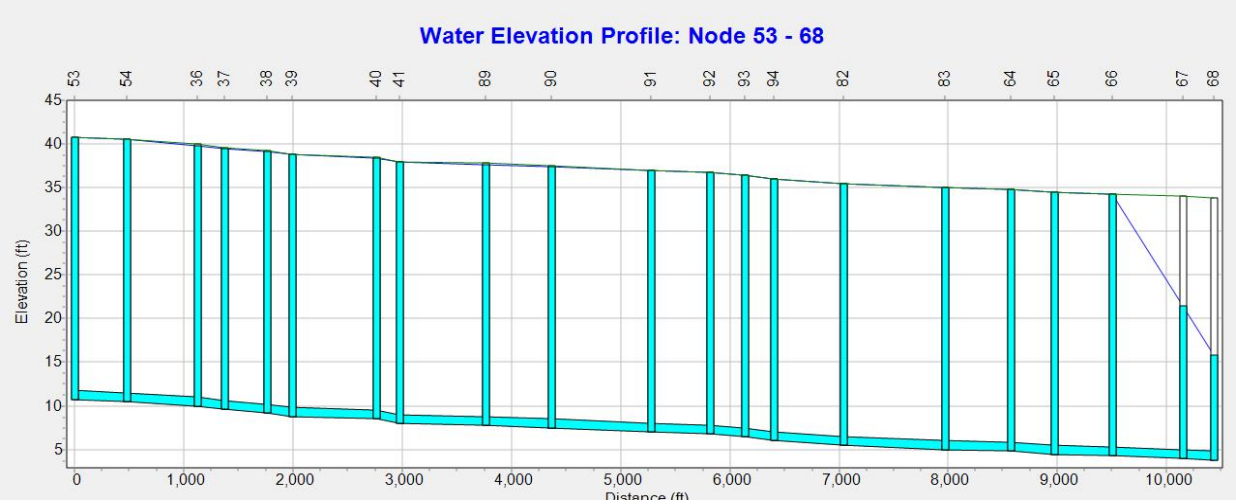

Figure 1B: Sample Profiles of the Storm B

Rank	Node ID	Continuity Error (%)	Max Inflow (CFS)	Invert Elev. (m)	Interpretation
1	61	1.34	898.76	5.20	Slight imbalance; indicates local surcharge zone but hydraulically stable
2	42	1.23	2,138.44	8.40	Minor continuity deviation; sustained pressurization rather than transient shock
3	35	1.21	1,372.39	6.00	Prolonged surcharge; relatively stable HGL despite high inflow
4	101	1.17	1,499.32	6.20	Minor storage/inflow imbalance; downstream bottleneck effects
5	90	1.12	3,569.56	7.50	Low error; acceptable numerical performance even under extended loading

Table 3.4: Nodes with Highest Continuity Errors (Storm B)

Rank	Link ID	From Node	To Node	Instability Index	Length (m)	Slope (%)	Max Flow (CFS)	Characteristic
1	8	37	38	43	389	0.1028	2,359	Strong backwater effects; sustained pressurization of upstream reservoir

2	7	36	37	42	244	0.1639	2,594	Steep conduit but insufficient capacity; momentum-driven oscillations
3	9	38	39	42	233	0.1717	3,570	Highest single-link flow; extreme backwater propagation
4	75	40	41	41	205	0.2439	4,160	Steep, short link but limited downstream capacity; downstream bottleneck
5	74	102	95	38	120	0.1833	1,197	Steep link near secondary outfall; pressure cycling at outlet interface

Table 3.5: Conducts with Highest Instability Index (Storm B)

Node ID	Non-Converging Time Steps (%)	Max Depth (m)	Implication
80	44.86	0.00	Persistent surcharge; outlet orifice creates backwater instability
69	44.86	0.00	High inflow volume relative to downstream capacity; repeated pressure adjustment
81	44.86	0.00	Node in chronic surcharge corridor; solver repeatedly adjusts HGL
72	39.17	3.80	Moderate solver difficulty: extended pressurization creates momentum coupling challenges
73	24.10	3.20	Minor instability; less critical than top nodes

Table 3.6: Nodes with Highest Non-Convergence Frequency (Storm B)